Supporting information

Carrier Doping Modulate Magnetoelectronic, and Magnetic Anisotropic Properties of Two-Dimensional MSi_2N_4 (M = Cr, Mn, Fe, and Co) Monolayers

Ziyuan An,[†] Linhui Lv,[†] Ya Su,[ξ*] Yanyan Jiang,[‡] Zhaoyong Guan[†§*]

[†]Key Laboratory of Colloid and Interface Chemistry, Ministry of Education, School of Chemistry and Chemical Engineering, Shandong University, Jinan, Shandong 250100, P. R. China

[ξ]School of Electrical Engineering, Shandong University, Jinan, Shandong 250100, P. R. China

[‡]Key Laboratory for Liquid-Solid Structural Evolution & Processing of Materials (Ministry of Education), School of Materials Science and Engineering, Shandong University, Jinan, Shandong, 250061, P. R. China

[§]School of Chemistry and Chemical Engineering, Shandong University, Jinan 250100, P. R. China

The Effective Onsite Coulomb Interaction Parameters (U) and the Exchange Interaction Parameters (J_0). The U are set to be 4.6 eV ($CrSi_2N_4$ and $MnSi_2N_4$), 6.0 eV ($FeSi_2N_4$), 7.6 eV ($CoSi_2N_4$). The J_0 are set to be 0.6 eV ($CrSi_2N_4$, $MnSi_2N_4$ and $CoSi_2N_4$), 0.5 eV ($FeSi_2N_4$), respectively. Therefore, the effective U_{eff} ($U_{\text{eff}} = U - J_0$) are set as 4.0 eV ($CrSi_2N_4$ and $MnSi_2N_4$),[1, 2] 5.5 eV ($FeSi_2N_4$),[3] 7.0 eV ($CoSi_2N_4$)[4, 5].

The Geometry of MSi_2N_4. The Geometries of MSi_2N_4 monolayers (MLs) have been optimized. MSi_2N_4 MLs are D_{3h} space group. The optimized lattices of MSi_2N_4 MLs are 2.875 ~ 2.920 Å. As a comparison, that of $MoSi_2N_4$ ML is 2.91 Å, which is found in the following paper (Mortazavi, B.; Javvaji, B.; Shojaei, F.; Rabczuk, T.; Shapeev, A. V.; Zhuang, X. Y., Exceptional Piezoelectricity, High Thermal Conductivity and Stiffness and Promising Photocatalysis in Two-Dimensional $MoSi_2N_4$ Family Confirmed by First-Principles. *Nano Energy* **2021**, *82*, 105716.). All of the MSi_2N_4 two-dimensional crystals belong to the hexagonal system, their lattice constants are 90°, 90°, 120°, respectively.

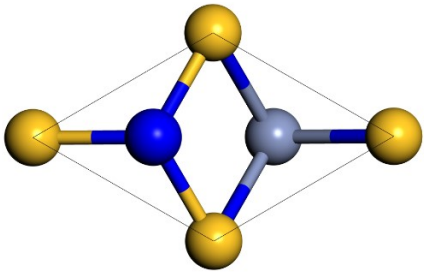

Fig S1. Calculated Geometries of MSi_2N_4 (M = Cr, Mn, Fe, and Co). The grey, ashen and blue balls in the figure present M, Si, N atoms.

Spin Charge Densities of MSi_2N_4. The spin charge densities of 1 × 1 × 1 cells of MSi_2N_4 MLs show that there are several single electrons occupying the M atom's orbitals. The single electrons result from electron transfer from the M atom to Si and N atoms. The spin charge densities are calculated with HSE06 functional.

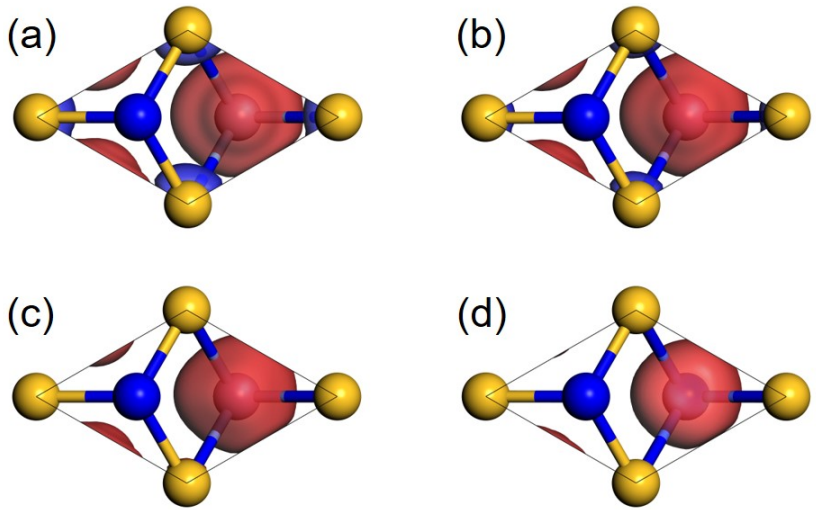

Fig S2. Spin charge densities of (a) $CrSi_2N_4$, (b) $MnSi_2N_4$, (c) $FeSi_2N_4$ and (d) $CoSi_2N_4$. The isovalue is 0.10 e/Å^3 in (a) - (d). Red and blue colors in the 1 × 1 × 1 cell represent spin-α and spin-β electrons, respectively.

Band Structures of Unit Cells of MSi_2N_4 MLs. The band structure and partial density of state (PDOS) of MSi_2N_4 are calculated, as shown in Fig S3a-d. This figure shows that the unit cells of the $CrSi_2N_4$ and $CoSi_2N_4$ MLs are the HMs while the $MnSi_2N_4$ and $FeSi_2N_4$ MLs are the semiconductors.

For $CrSi_2N_4$ and $CoSi_2N_4$, some bands occupied by spin-α electrons cross the Fermi energy, making them metallic, while the spin-β electrons of $CrSi_2N_4$ and $CoSi_2N_4$ MLs behave like semiconductive properties. Thus, $CrSi_2N_4$ and $CoSi_2N_4$ MLs are HM. The Fermi-level is partially occupied by the spin-α electrons. For spin-β electrons in $CrSi_2N_4$ and $CoSi_2N_4$ MLs, the valance band maximum (VBM) of $CrSi_2N_4$ and $CoSi_2N_4$ is located at the Γ point, while the conduction band minimum (CBM) is located at the F and K points, respectively. There are about a bandgap of 3.661 eV and 2.021 eV in the $CrSi_2N_4$ and $CoSi_2N_4$ MLs' spin-β state, as shown in Fig S3a, d, respectively. HM could provide 100% spin-polarized current, so the $CrSi_2N_4$ and $CoSi_2N_4$ MLs could work as the HMs. It means that they have a wide application in the spin transport device and spin injection.

For $MnSi_2N_4$ and $FeSi_2N_4$ MLs, they are semiconductors, and the VBMs are located at the Γ point, as shown in Fig S3b, c, respectively. The CBM of $MnSi_2N_4$ is located at

the point between the K and Γ points, and the CBM of $FeSi_2N_4$ is located at the K point. The calculated band gaps of $MnSi_2N_4$ and $FeSi_2N_4$ are 0.427 and 0.282 eV, respectively. The band structures indicate that the $MnSi_2N_4$ and $FeSi_2N_4$ MLs' orbitals near the Fermi-level are occupied by the spin-α electrons, shown in Fig S3b, c, respectively. The orbital projected band structures of $MnSi_2N_4$ and $FeSi_2N_4$ MLs are calculated, shown in Fig S3a-d. Taking $FeSi_2N_4$ ML as an example, the states near the Fermi-level are mainly contributed by N's p orbitals, while the states around the Fermi-level are partially contributed by the Fe's d_{yz} and d_{xz} orbitals, as shown in Fig S4c, S7c, and S8, respectively. Moreover, these orbitals are all occupied by the spin-α electrons.

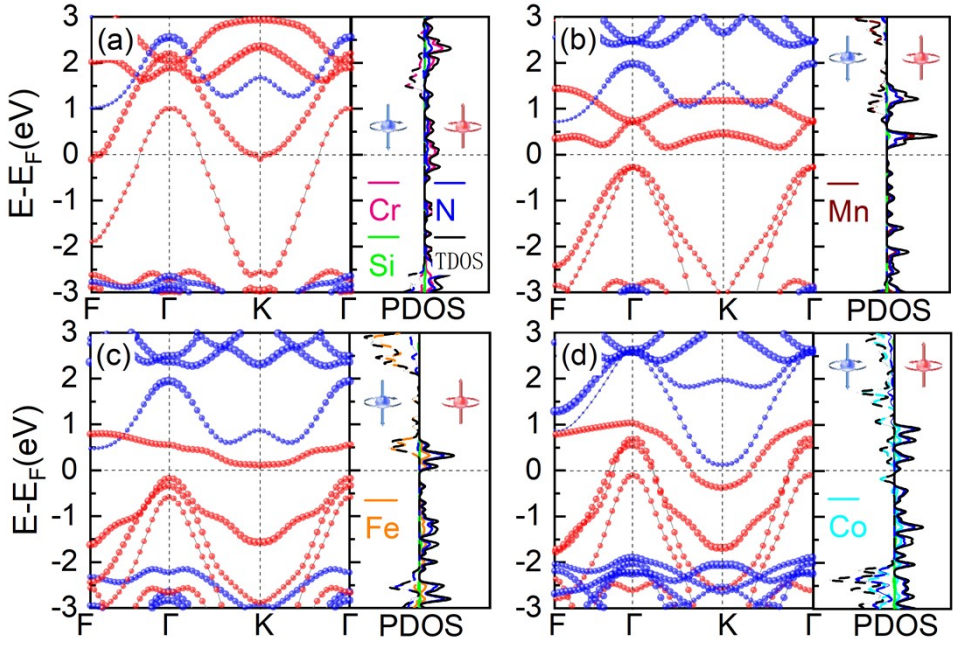

Fig S3. Band structures of FM orders of MSi_2N_4 MLs with (a) $CrSi_2N_4$, (b) $MnSi_2N_4$, (c) $FeSi_2N_4$, and (d) $CoSi_2N_4$ are calculated with HSE06 functional.

The Orbital Projected Band Structures of the $MnSi_2N_4$ MLs. The p-orbital and d-orbital projected band structures of the HMs ($CrSi_2N_4$ and $CoSi_2N_4$ MLs) are calculated, shown in Fig S4a-d. Taking $CrSi_2N_4$ ML as an example, the states near the Fermi-level are contributed by N's p_y orbitals, Cr's d_{xy} and $d_{x^2-y^2}$ orbitals which are occupied by the spin-α electrons, as shown in Fig S4a, S6a-c, and S7a, respectively.

The orbital projected band structures of the semiconductors ($MnSi_2N_4$ and $FeSi_2N_4$

MLs) are also calculated, shown in Fig S3a-d. Taking $FeSi_2N_4$ ML as an example, the states near the Fermi-level are mainly contributed by N's *p* orbitals, while the states around the Fermi-level are partially contributed by the Fe's d_{yz} and d_{xz} orbitals, as shown in Fig S4c, S7c, and S8, respectively. Moreover, these orbitals are all occupied by the spin-α electrons.

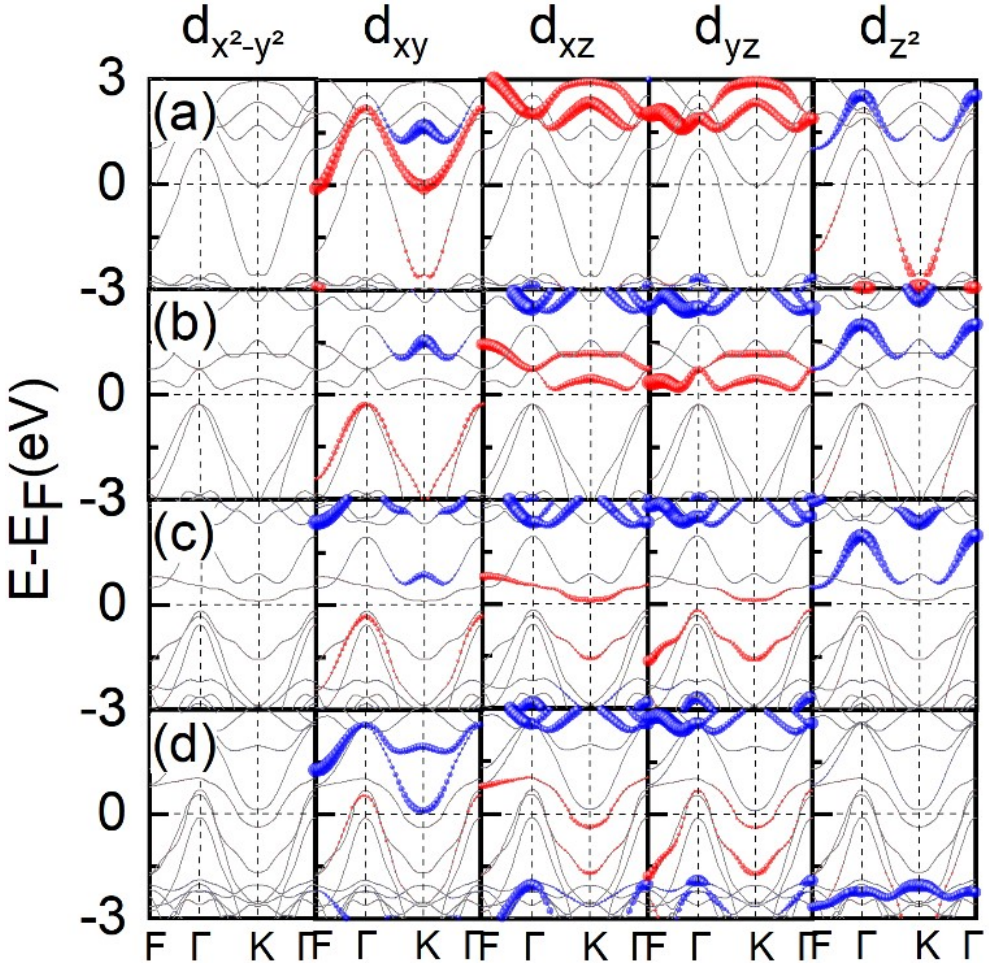

Fig S4. MSi_2N_4 MLs' d-orbital projected band structures. The red and blue lines with dots in every thumbnail image present $d_{x^2-y^2}$, d_{xy}, d_{xz}, d_{yz}, and d_{z^2} atomic orbitals of (a) $CrSi_2N_4$, (b) $MnSi_2N_4$, (c) $FeSi_2N_4$, (d) $CoSi_2N_4$ from left to right. The Fermi-level is set 0.

3*d*-orbital IDOS of MSi_2N_4. The 3*d*-orbital IDOS of MSi_2N_4 MLs are calculated with HSE06 functional. The Fig S5 shows that the numbers of spin-β valence electrons of the MSi_2N_4 MLs are 0.92 (Cr), 0.79 (Mn), 1.16 (Fe), and 2.12 (Co), respectively. This

figure shows that these d_{yz} and d_{xz} atomic orbitals are degenerate. These d_{xy} and $d_{x^2-y^2}$ atomic orbitals are also degenerate.

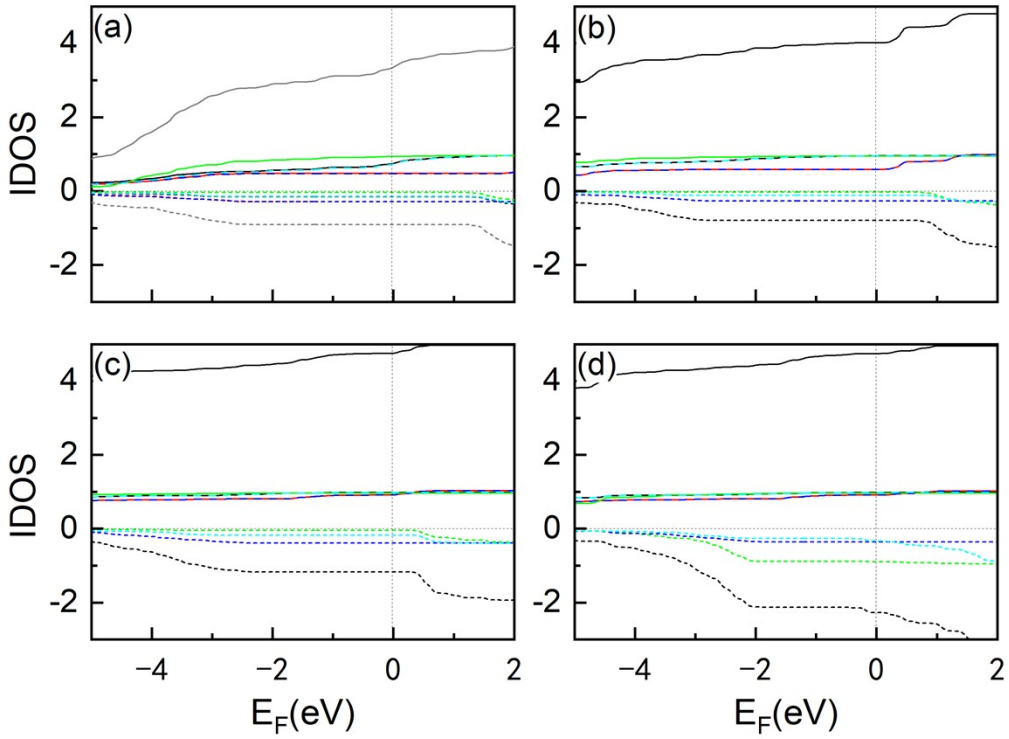

Fig S5. (a) $CrSi_2N_4$, (b) $MnSi_2N_4$, (c) $FeSi_2N_4$, and (d) $CoSi_2N_4$ MLs' 3*d*-orbital IDOS. The black, red, green, blue, cyan, and grey lines in the figure present d_{xy}, d_{yz}, d_{z^2}, d_{xz}, $d_{x^2-y^2}$, and d atomic orbitals IDOS. The solid and dash lines in the figure present spin-α and spin-β electrons.

The p-orbital Projected Band Structure. The p-orbital projected band structures of $CrSi_2N_4$ and $MnSi_2N_4$ in Fig S6 show that the states around the Fermi-level are mainly contributed by the p_y orbitals, respectively. The band structures and electronic properties are related to the type of the MSi_2N_4. There are electronic states at Fermi-level of $CrSi_2N_4$ while there aren't for the $MnSi_2N_4$. Thus, the $MnSi_2N_4$ is the semiconductor, but the $CrSi_2N_4$ isn't. The band structures are calculated with HSE06 functional.

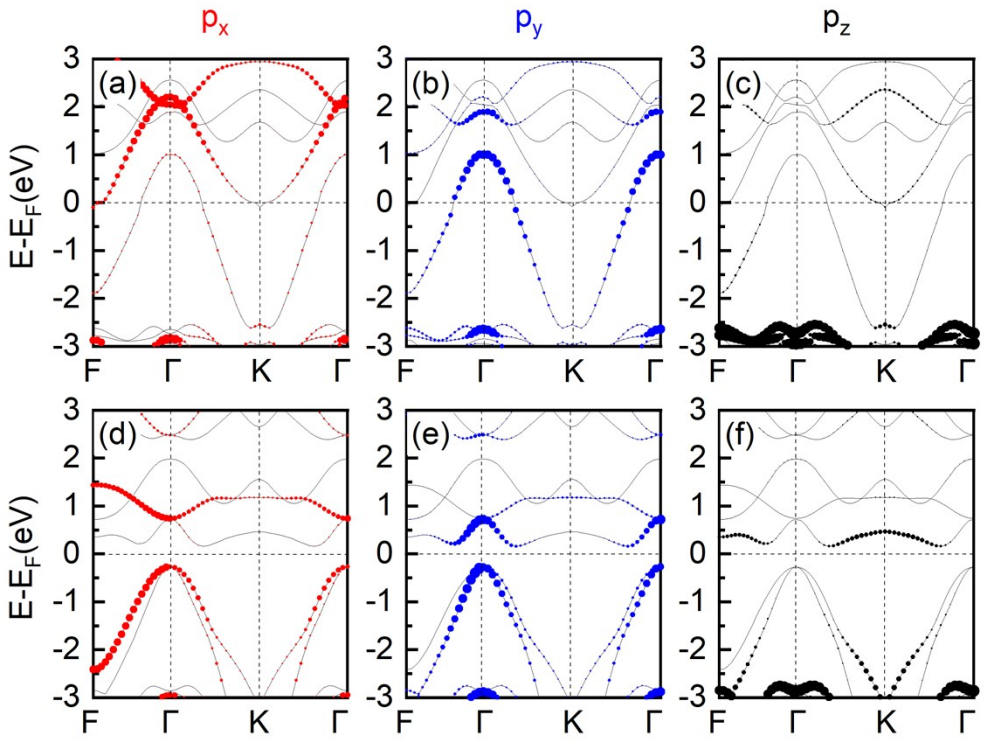

Fig S6. (a-c) $CrSi_2N_4$ and (d-f) $MnSi_2N_4$ MLs' p-orbital projected band structures. The red, blue, black points in lines present (a, d) p_x, (b, e) p_y and (c, f) p_z atomic orbitals of $CrSi_2N_4$ and $MnSi_2N_4$ MLs.

The d-orbital Partial Density of the States of MSi_2N_4. The d-orbital partial density of the states of MSi_2N_4 MLs are calculated with HSE06 functional. The Fig S7 shows that states near the Fermi-level are mainly contributed by spin-α electrons of d_{xy} and $d_{x^2-y^2}$ atomic orbitals ($CrSi_2N_4$), spin-α electrons of d_{yz} and d_{xz} atomic orbitals ($MnSi_2N_4$ and $FeSi_2N_4$), spin-β electrons of d_{xy} and $d_{x^2-y^2}$ atomic orbitals ($CoSi_2N_4$).

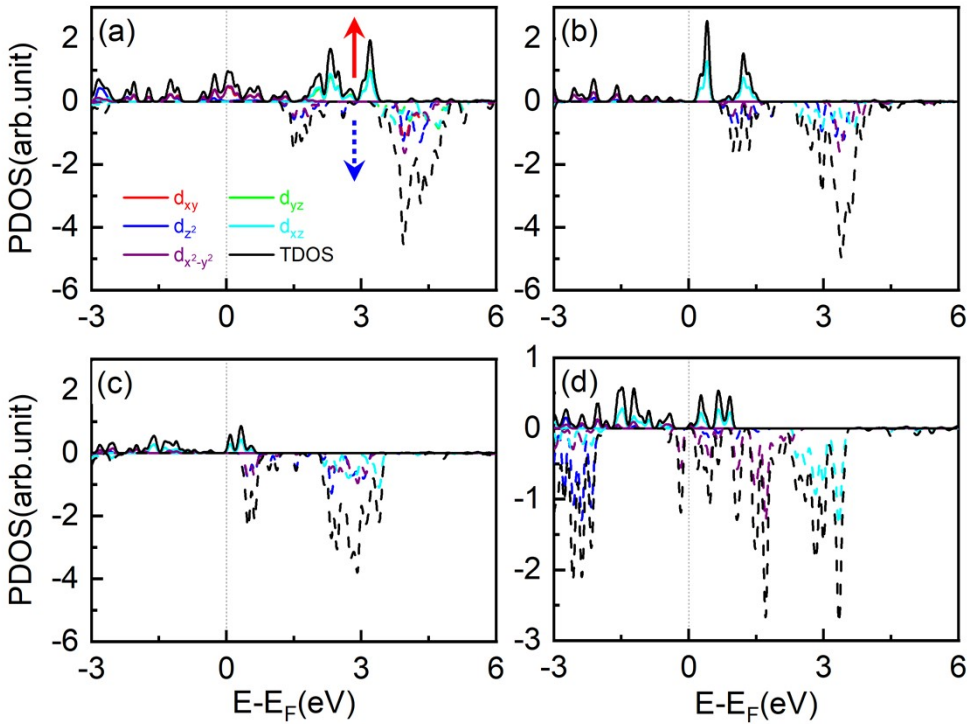

Fig S7. (a) $CrSi_2N_4$, (b) $MnSi_2N_4$, (c) $FeSi_2N_4$, and (d) $CoSi_2N_4$ MLs' d-orbital projected band structures. The red, green, blue, cyan, purple, black lines in the figure above present d_{xy}, d_{yz}, d_{z^2}, d_{xz}, and $d_{x^2-y^2}$ atomic orbitals. The solid and dash lines in the figure above present spin-α and spin-β electrons.

Orbital Projected Band Structures of $FeSi_2N_4$. The band structures of $FeSi_2N_4$ shown in Fig S8 reveal that states near the Fermi-level are mainly contributed by spin-β electrons of Fe atomic orbital and spin-α electrons of N atomic orbital. The valance band maximum (VBM) of $FeSi_2N_4$ is located at Γ point, whose value is -0.171 eV. The conduction band minimum (CBM) of it is located at K points, whose value is 0.110 eV. The gap of $FeSi_2N_4$ is 0.282 eV. Both of the VBM and CBM are occupied by the spin-α electrons, as shown in Fig S8. The band structure is calculated with HSE06 functional.

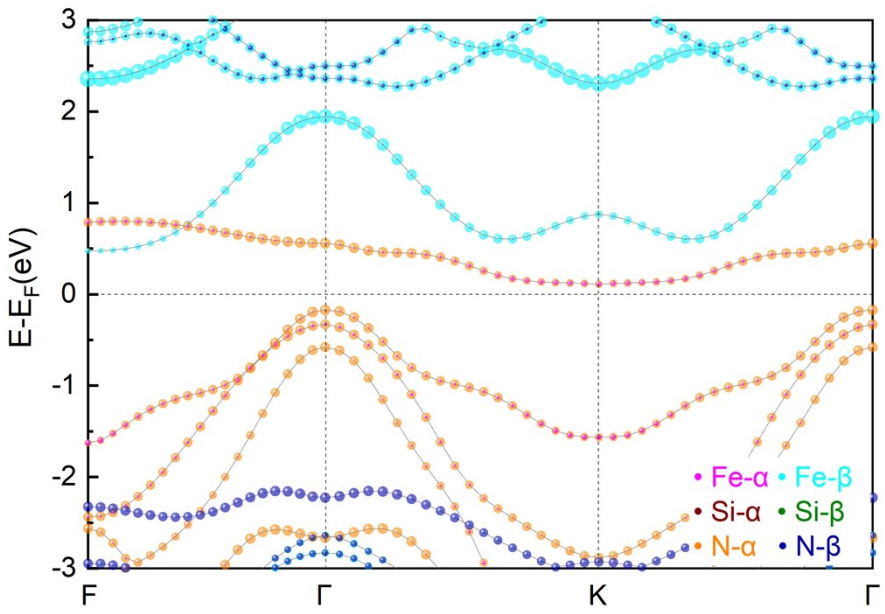

Fig S8. Band structure of $FeSi_2N_4$ ML. The dots colored by carmine, wine red and orange present spin-α electrons' channel of Fe, Si and N by order. The dots colored by cyan, olive green and royal blue present spin-β electrons' channel of Fe, Si and N by order.

Superexchange Interactions in MSi_2N_4 MLs. The following figure shows that direct exchange interaction, superexchange interaction and the mechanism of superexchange. $CrSi_2N_4$ is taken as an example. According to the data in the paper, direct exchange interaction plays a major role in undoped system. The format of this figure refers to this paper (Jiang, X.; Liu, Q. X.; Xing, J. P.; Liu, N. S.; Guo, Y.; Liu, Z. F.; Zhao, J. J., Recent Progress on 2D Magnets: Fundamental Mechanism, Structural Design and Modification. Appl Phys Rev 2021, 8, 031305.).

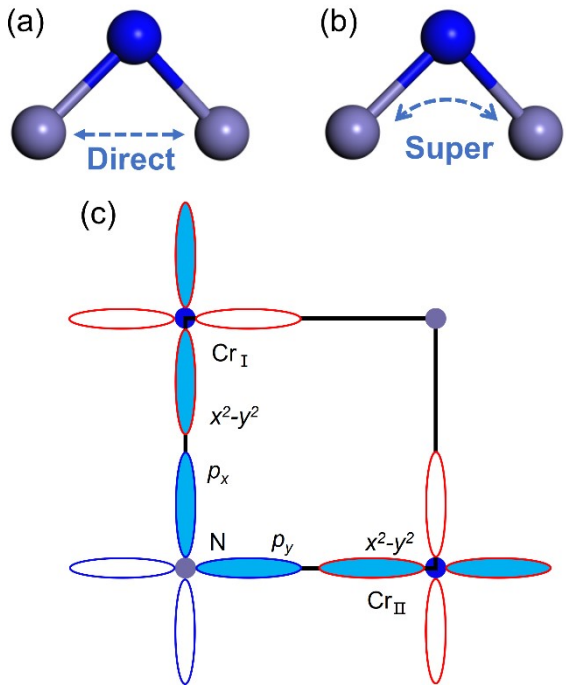

Fig S9. (a) Direct exchange interaction, (b) superexchange interaction and (c) schematic structure of the superexchange interaction in $CrSi_2N_4$ ML.

The d-orbital Partial Density of the States of MSi_2N_4 with AFM Orders. The d-orbital partial density of the states of 2×2×1 cells of MSi_2N_4 MLs with AFM orders are calculated with HSE06 functional. The Fig S11 shows that states near the Fermi-level are mainly contributed by d_{xy} and $d_{x^2-y^2}$ atomic orbitals ($CrSi_2N_4$, $MnSi_2N_4$ and $CoSi_2N_4$), d_{yz} and d_{xz} atomic orbitals ($FeSi_2N_4$). Especially, the d-orbital partial density of the states of $MnSi_2N_4$ and $FeSi_2N_4$ MLs are highly symmetric along Fermi-level.

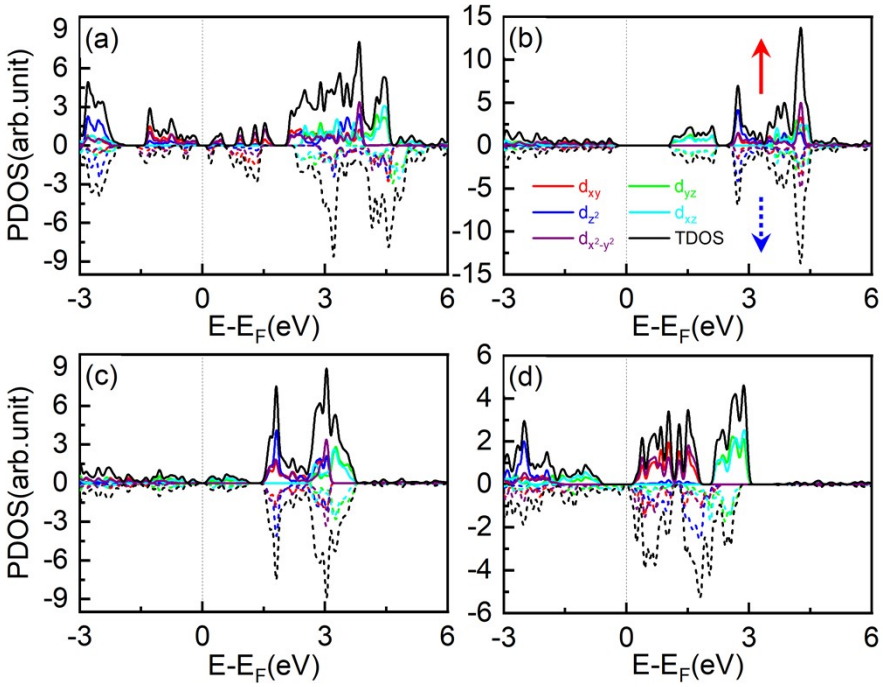

Fig S10. MSi_2N_4 (M = (a) Cr, (b) Mn, (c) Fe, and (d) Co) MLs' d-orbital projected band structures. The red, green, blue, cyan, purple, black lines in the figure above present d_{xy}, d_{yz}, d_{z^2}, d_{xz}, and $d_{x^2-y^2}$ atomic orbitals. The solid and dash lines in the figure above present spin-α and spin-β electrons.

Electronic Properties of Doped $CoSi_2N_4$. This picture tells us that both positive (+0.4 and +0.6 *e*) and negative (-0.4 and -0.6 *e*) charges doped $CoSi_2N_4$ are HM. All of the states of the Fermi-level of the doped $CoSi_2N_4$ ML are mainly contributed by the spin-α electrons but except -0.4 *e* charges doped $CoSi_2N_4$ ML. It indicates that the charge doping could change the electronic structures of the MSi_2N_4 MLs.

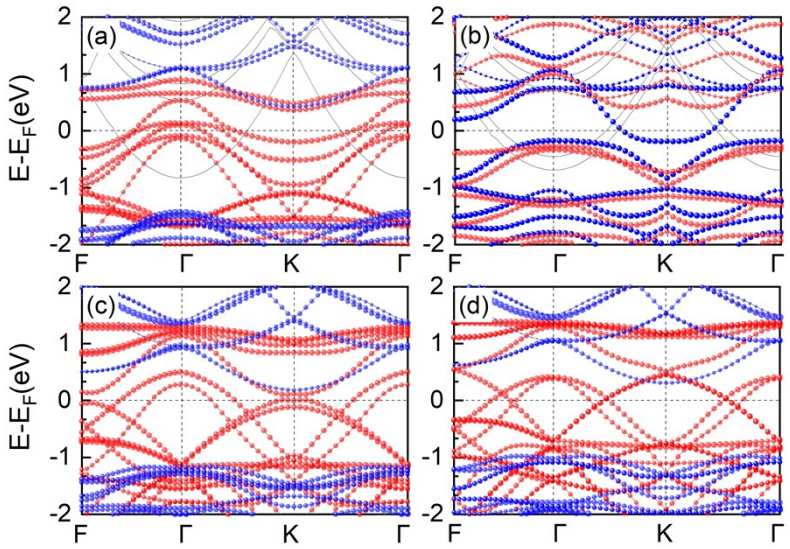

Fig S11. Band structures of (a) -0.6, (b) -0.4, (c) +0.4 and (d) +0.6 charges doped $CoSi_2N_4$. The dots colored by red and blue present spin-α and spin-β electrons' channel.

Snapshots of AIMD. Ab initio molecular dynamics (AIMD) simulation is used in calculating the constant moles–volume–temperature (NVT) ensemble, which is with Nosé–Hoover thermostat. Some key paraments are set as followed: the simulated temperature is set as 300 K. The time step is 1 fs, and the total step is 100000. Thus, the total time is 10 ps. A 2 × 2 × 1 cell is applied in the simulation. Fig S13 shows the snapshots of MSi_2N_4 with AIMD. These snapshots record the geometries of MSi_2N_4 at time of 2, 4, 6 and 8 ps, respectively. In conclusion, there is no obvious distortion and the complete structures of MSi_2N_4 could be kept during the simulation.

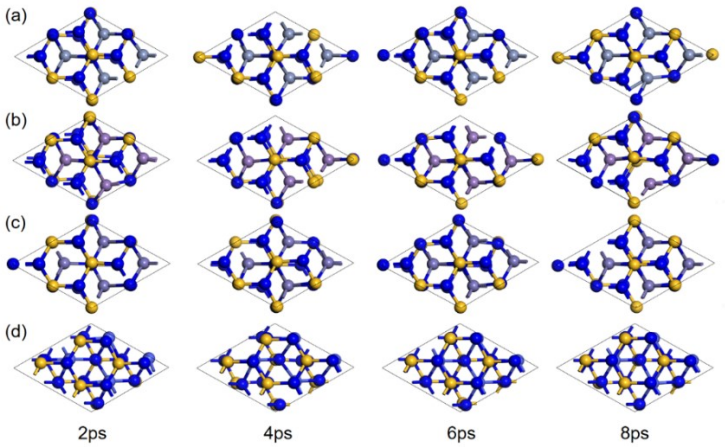

Fig S12. Snapshots of (a) $CrSi_2N_4$, (b) $MnSi_2N_4$, (c) $FeSi_2N_4$, (d) $CoSi_2N_4$ taken at 2, 4, 6, 8 ps. The NVT of simulation is set as 300K.

Contribution Values of Different Atoms of Doped $CrSi_2N_4$. The following table shows the contribution values of three different atoms Cr, Si and N to the MAE of doped $CrSi_2N_4$ ML. The data shown in the following table supports the conclusion that the MAE of doped $CrSi_2N_4$ ML is mainly attributed by Cr atom.

Table S1. Specific Contribution Values of Different Atoms of $CrSi_2N_4$ with Different Doped Charges

Doped charges	Atom	contribution value (meV)
+0.6 *e*	Cr	-0.0179
	Si	0
	N	-0.0036
+0.7 *e*	Cr	0.0082
	Si	-0.0002
	N	-0.0056
+0.9 *e*	Cr	0.0196
	Si	-0.0006
	N	-0.0042

Chemical Bonds and Their Impact in the Magnetic Properties. There are electrons transfers from M atom to the nearby Si and N atoms due to the electronegativity difference. Besides, the electron transfers make some *d* orbitals are occupied by just a single electron. Their spin charge densities are shown in Fig S2a-d. Each M atom has a magnetic moment (MM) of 2.56 (M = Cr), 3.31 (Mn), 3.84 (Fe), and 2.51 (Co) μ_B, respectively, while the MMs of silicon and nitrogen atoms are closed to 0 μ_B.

M atom is bonded with silicon and nitrogen atoms. Due to the electronegativity difference between atoms, there are charge transfers. The valence electron numbers of a M atom are 6.00 (Cr), 7.00 (Mn), 8.00 (Fe), and 9.00 (Co), respectively. The Bader

charge analysis finds that the numbers of valence electrons per atom are 4.48 (Cr), 5.44 (Mn), 6.50 (Fe), and 7.87 (Co) in MSi_2N_4 MLs, respectively. These valence electrons mainly fill the 3*d* orbitals. According to the integrated density of states (IDOS), the numbers of spin-β valence electrons of the MSi_2N_4 ML are 0.92 (Cr), 0.79 (Mn), 1.16 (Fe), and 2.12 (Co), respectively, as shown in Fig S5a-d. The estimated values of M/MMs of the MSi_2N_4 MLs are equal to the difference between the numbers of spin-α and spin-β valence electrons. These numbers can't exceed 5 as the limited number of 3*d* orbitals. So, based on the above results, it can be estimated that the M/MMs are 2.64 (Cr), 2.86 (Mn), 3.84 (Fe), and 2.88 (Co) μ_B, respectively. They are close to the M/MMs calculated with HSE approaches, especially for $CrSi_2N_4$, $FeSi_2N_4$, and $CoSi_2N_4$ MLs. Given the Bader charge analysis and the IDOS, the charge transfers during the bonding process could well explain the M/MMs calculated with HSE approaches.

Reference

1. R. Ponce-Perez, K. Alam, G. H. Cocoletzi, N. Takeuchi and A. R. Smith, *Appl. Surf. Sci.*, 2018, **454**, 350-357.
2. S. M. Hailemariam, *Adv. Condens. Matter Phys.*, 2020, **2020**, 9635917.
3. Z. Y. Guan and S. Ni, *J. Phys. Chem. C*, 2021, **125**, 16700-16710.
4. C. M. Zhang, L. Zhang, C. Tang, S. Sanvito, B. Zhou, Z. Y. Jiang and A. J. Du, *Phys. Rev. B*, 2020, **102**, 134416.
5. S. J. Gong, C. Gong, Y. Y. Sun, W. Y. Tong, C. G. Duan, J. H. Chu and X. Zhang, *Proc. Natl. Acad. Sci.*, 2018, **115**, 8511-8516.